International Journal of Biological Macromolecules 117 (2018) 134–143

Contents lists available at ScienceDirect

International Journal of Biological Macromolecules

journal homepage: http://www.elsevier.com/locate/ijbiomac

Nano-magnetic cross-linked enzyme aggregates of naringinase an efficient nanobiocatalyst for naringin hydrolysis

Homa Torabizadeh *, Mohaddeseh Mikani

Iranian Research Organization for Science and Technology (IROST), Department of Chemical Technologies, Food Science and Technology Group, Mojtama Asre Enghelab Building, Shahid Ehsanirad Street, 33535111 Tehran, Iran

ARTICLE INFO

Article history:
Received 23 April 2018
Received in revised form 15 May 2018
Accepted 22 May 2018
Available online 23 May 2018

Keywords:
Naringinase immobilization
MN-NGase-CLEAs
Naringin hydrolysis

ABSTRACT

In this research, the preparation and characterization of a novel biocatalyst comprising nano-magnetic cross-linked enzyme aggregates of naringinase (NM-NGase-CLEAs), which was covalently bounded to lysine-assisted magnetic nanoparticles, were studied. The Schiff base formed between ε-amino groups of the lysine residues and aldehyde groups of glutaraldehyde was reduced by ascorbic acid. Among the six different precipitants, tert-butanol performed the best for naringin hydrolysis. The optimal conditions for the immobilization process required 10 mM glutaraldehyde, 1:10 ratio of lysine/enzyme, and 3 h crosslinking at 3–4 °C. The morphology of the NM-NGase-CLEAs implied a non-uniform, semi-pyramid and semi-cubic rods. The dynamic light scattering (DLS) results showed that the nanomagnetite particle size was around 81.9–96.5 nm, with a polydispersity index (PDI) of 0.238. After NM-NGase-CLEAS formation, the particle size was reduced to around 13.2–15.3 nm, with PDI of 0.177, respectively. Moreover, the ζ-potential of −28 mV also confirms the improvement of CLEAs stability. The NM-NGase-CLEAs kept 73% of its original activity after 10 cycles, which proposes strong operational stability. In conclusion, the NM-NGase-CLEAs are thermo-stable, reusable, and efficient nanobiocatalyst for debittering of citrus juices.

1. Introduction

Naringinase is a hydrolytic multienzyme complex, which consists of α-L-rhamnosidase (EC 3.2.1.40) and β-D-glucosidase (EC 3.2.1.21) activities. Alpha-rhamnosidase catalyzes the hydrolysis of naringin (naringenin 7-rhamnoglucoside) into rhamnose and prunin (4,5,7-trihydroxy flavanone-7-glucoside); the prunin is altered to naringenin (4,5,7-trihydroxy flavanone) and glucose by the β-D-glucosidase activity at the same time [1,2]. This enzyme activity attracts growing biotechnological interest, owing to its role in debittering of citrus fruit juices [1]. Naringinase also finds applications in the fabrication of glycopeptide antibiotics, deglycosylation of flavonoids, and gellan depolymerisation [2]. In addition, its hydrolysis products (rhamnose, prunin and naringenin) display biological activities and can be employed as starting materials for the synthesis of substances used in pharmaceutics, food technology, and cosmetics [3]. In the food processing industry, the rhamnosidases have been employed primarily for debittering of citrus juices. The presence of bitterness is a major restriction in the commercial acceptance of juices [4]. Both free and immobilized α-L-rhamnosidases from various microorganisms have been explored for naringin hydrolysis. Immobilized enzymes are preferred over free enzymes in large-scale applications, due to improved enzyme stability and reusability; furthermore, loss of enzyme activity during the immobilization and reaction process, large mass transfer resistance between the enzyme and substrates, and the inconvenience of selecting the proper immobilization technique are the drawbacks of their use [5]. Recently, several studies have been performed on the progress of immobilization techniques and materials [6]. Jiang et al. immobilized successfully horseradish peroxidase and α-amylase by cross-linked enzyme aggregates (CLEAs) method onto an inverse opal [7]. Gao et al. immobilized lipase by monodisperse core-shell magnetic organosilica nanoflowers [8]. Jiang et al. prepared CLEAs of lipase in three-dimensionally ordered macroporous silica materials [9] also, Cruz-Izquierdo et al. immobilized lipase by magnetic CLEAs method [10]. Moreover, Cui et al. prepared immobilized phenylalanine ammonia lyase via mesoporous CLEAs-silica composite microparticles for enhancing of enzyme activity and stability [11], as well as, cutinase was immobilized on amino-functionalized magnetic supports by CLEAs method for its use in bio-degradation of polycaprolactone by Singh [12]. Samoylova et al. fabricated esterase CLEAs for application in malathion removal from municipal wastewater [13]. Martínez-Moñino et al. prepared nicotinic acid mononucleotide deamidase CLEAs to obtain highly valuable NAD^+-boosters [14]. Many strategies have been recently employed to immobilize naringinase. Nanotechnology is at an innovative stage of knowledge and technical development, with possible applications in numerous spheres such as

* Corresponding author.
E-mail address: htoraby@alumni.ut.ac.ir (H. Torabizadeh).

https://doi.org/10.1016/j.ijbiomac.2018.05.162
0141-8130/

electronics, mechanics, metallurgical engineering, and chemistry. Nanometer-sized particles (NPs) have rapidly and broadly progressed [15]. Iron oxide nanoparticles have attracted much interest for biomedical applications, owing to their outstanding characteristics comprising superparamagnetism and low toxicity. In particular, solutions of maghemite (γ-Fe_2O_3) or magnetite (Fe_3O_4) particles in the diameter of 7.5–100 nm have displayed promise as magnetic fluids for targeted drug delivery. Their potential applications cover several fields especially in biomedical applications [16,17]. For in vivo applications, the magnetic nanoparticles (MNPs) can be coated with a biocompatible and diamagnetic material (such as organic polymers or silica shells) to inhibit the formation of large aggregates of MNPs and to facilitate functions such as drugs attachment [1,18]. The binding efficiency of enzyme was improved by high specific surface of MNPs, while the selective recovery of the biocatalyst using a magnet was permitted by the support of its superparamagnetic behavior [19,20]. The formation of CLEAs of naringinase with glutaraldehyde is a simple technique, which does not need to employ highly pure enzymes [10,21]. CLEAs have appeared as a biocatalyst design for immobilization in an interesting way. Moreover, since aggregation can be employed in enzyme purification and CLEAs fabrication, this method may integrate in a single or multiple operation consisting of enzyme purification and immobilization. This new generation of biocatalysts, CLEAs, in addition to illustrating good mechanical stability, can be highly active, since they do not comprise large amounts of foreign particulate non-enzymatic material and may have improved stability. They have a broad scope and afford robust, recyclable catalysts that illustrate high activity retention, improved thermal stability, better tolerance to organic solvents, and increased resistance to autoproteolysis owing to the rigidification of the enzyme tertiary structure [22–25]. The CLEAs technique presents many advantages in numerous applications, as it is simple and amenable to rapid optimization, leading to low costs and short time-to-market processes [26]. In this study, a new method for the preparation of NM-CLEAs of naringinase has been developed. This method comprises the nano cross-linking of free naringinase in a solvent and the bonding of nano-CLEAs to aminated MNPs (lysine-assisted Fe_3O_4) by glutaraldehyde [27] and the reduction of the Schiff base formed between ε-amino groups of the lysine residues and aldehyde groups of glutaraldehyde by safe and efficacious reducing agents such as ascorbic acid (vitamin c) [28]. The resulting NM-CLEAs fulfill the main benefits of magnetic biocatalysts and CLEAs, as they illustrate improved thermal and storage stabilities, and can be reused after their recovery from the reaction mixture with a magnet [29]. In this research, the problems encountered with using the CLEAs such as mass transfer reduction, loss of ultra-fine aggregated enzymes during recovering of CLEAs from the reaction medium [30], washing and reusing, have been resolved.

2. Experimental

2.1. Materials

Viscozyme L produced from a selected strain of *Aspergillus aculeatus* was supplied by Novozymes (Bagsvaerd, Denmark). Naringin, glutaraldehyde (25% v/v in water), sodium potassium tartrate, 3,5 dinitrosalicylic acid, $FeCl_2$, $FeCl_3$, D(+) glucose, L-lysine monohydrochloride (>99%), and ascorbic acid were purchased from Merck. Bovine serum albumin (BSA) was obtained from Fluka company. Coomassie brilliant blue (G-250) was purchased from GE Healthcare (Uppsala, Sweden). All other chemicals were supplied by Merck (Darmstadt, Germany).

The surface analysis was done using a Tescan Mira II FE-SEM (USA) at a voltage of 20.0 kV, after coating the samples with a thin layer of gold by magnetron sputtering. Perkin Elmer Lambda 25UV/VIS spectrophotometer (USA) was employed for absorbance intensity in cells with 1 cm path length against the blank. The infrared spectra of all formulations were obtained using Fourier transform infrared spectroscopy (FTIR-8300, Shimadzu, Japan). The DLS technique was broadly employed for sizing the nanomagnetite and naringinase nanomagnetic nano CLEAs in the liquid phase, applying a BI-200 SM Goniometer Version 2 (Brookhaven Instrument Corp., Holtsville, NY, USA). The light scattered by the nanoparticles was detected at 173° in dynamic laser scattering. Besides, the zeta potential was determined by the DLS method and was employed to estimate the nanoparticle stability against aggregation. All values were expressed as mean ± standard deviation of the three replicate experiments.

2.2. Methods

2.2.1. Synthesis of magnetic nanoparticles

Nanomagnetite was fabricated by co-precipitation of iron salts in NaOH environment [31]. The co-precipitation method is the simplest chemical process and the most economical, efficient approach to acquire Fe_3O_4 nanoparticles. The MNPs were supplied by mixing $FeCl_3$ and $FeCl_2$ in 2:1 M ratio. The aqueous solutions of Fe^{2+} and Fe^{3+} were made in distilled water. The solution of NaOH was added dropwise to the mixture while keeping the pH at the range of 9.0 to 9.5. Black colored particles of iron oxide were precipitated in the solution at room temperature by strongly stirring with a mechanical stirrer in alkaline medium. Moreover, an N2 gas stream was constantly bubbled through all solutions during the process. The particles were isolated by high-speed centrifugalization at 11357 ×*g* for 20 min, washed with distilled water for 3 times. Lastly, the attained particles were dispersed in the distilled water by an ultrasonic bath [32,33]. The FE-SEM analysis was accomplished by EDX evaluation of the supplied MNPs.

2.2.2. Functionalization of magnetic nanoparticles by lysine addition

MNPs have a large surface area/volume ratio, which leads to particle aggregation; consequently, the surface energy decreases owing to strong magnetic attractions between particles, inhibiting particle dispersion in aqueous solutions. Some effective protection techniques such as coating were employed to overcome this limitation. Various materials have been involved in this process, such as polylysine, BSA, 3-aminepropyltrimethoxysilane (APTMS), 3-aminopropyl triethoxysilane (APTES) a toxic compound with health hazards [34]. In this research, lysine with reactive ε-NH2 groups was applied for coating the MNPs [35,36]. The appropriate amount of lysine was dissolved in 50 ml 100 mM sodium acetate buffers (pH 5.0); then, the water-based Fe_3O_4 MNP equal to the amount of lysine was injected to the lysine solution. After that, fast mechanical stirring was carried out for lysine binding directly onto Fe_3O_4 nanoparticles at room temperature. Then 24 h later, the Fe_3O_4@lysine nanoparticles acquired were separated centrifugally at 11357 ×*g* and washed with distilled water to eliminate the unreacted lysine as much as possible. Interaction between Fe_3O_4 and lysine should be carried out in reactive forms in aqueous solution. It is specified that, the zeta potential of Fe_3O_4 at pH of approximately 7.5–7.7 is around zero (isoelectric point) and the particles are aggregated [37,38]. Below this isoelectric point, the surface of MNPs is positively ($\equiv Fe\text{-}OH_2^+$) and above isoelectric point is negatively ($\equiv Fe\text{-}O^-$) charged respectively. In L-lysine structure there is an α-carboxyl group ($\text{-}COO^-$), an α-amino group (NH_3^+), and a side-chain amino group (NH_3^+). Depends on pH of the solution, the charged state of these groups is altered. The dissociation constants (pK_a) of the acidic carboxyl group and the basic amino groups are 2.2, 9.1 and 10.8, respectively [37,38].

Based on data reported by Viota et al. and Antal et al., the maximum adsorption of L-lysine onto magnetic nanoparticles are achieved when the pH of the solution is between 3 and 5 [37,38]. Since, our research is operated in 100 mM sodium acetate buffer pH 5.0, it is expected that, bonding between lysine and Fe_3O_4 is formed through negatively charged α-carboxyl group ($\text{-}COO^-$) of lysine and positively charged ($\equiv Fe\text{-}OH_2^+$) of nanomagnetite. In this way, the presence of free NH_3^+ groups on the surface of MNPs are conserved for conjugation with

naringinase CLEAs by reaction between glutaraldehyde (cross-linker) and accessible surface lysine amino groups of the enzyme.

2.2.3. Preparation of naringinase aggregates in precipitant agents

The aggregation was acquired by adding 100 μL enzyme solution and different concentrations (0.3–15 mg) of BSA and/or lysine to 900 μL of the precipitant (isopropanol, acetone, tert-butanol, acetonitrile, ethanol, and saturated ammonium sulfate). The naringinase aggregate suspension was completely shaken and preserved in ice for 20 min. Thereafter, the aggregated enzyme was separated from the solvents by 11,357 ×*g* centrifugation, and the enzyme activity assay was carried out by the DNS method.

2.2.4. Preparation of naringinase CLEAs

Cross-linking was carried out by the addition of a definite glutaraldehyde (25% v/v) amount after the precipitation step. Then, it was held at 2–4 °C for 4–12 h (overnight incubation). Afterwards, the CLEAs formed were separated from the supernatant, by centrifuging at 11357 ×*g* for 10 min, so the extra residual glutaraldehyde and solvents were eliminated. The supplied CLEAs were re-suspended in 2 mL 50 mM phosphate buffer (pH 7), then was separated by centrifuge and washed 3 times. Finally, the enzyme activity was measured.

2.2.5. Preparation of nano-magnetic CLEAs of naringinase

In order to obtain NM-NGase-CLEAs, MNPs@lysine was added to the enzyme/lysine at 1.7 folds of enzyme protein in the presence of precipitating agents (tert-butanol) in a final volume of 2 ml at room temperature, together with the addition of 1–100 mMol glutaraldehyde. Consequently, ultrasonic bath (200 Hz) was applied for directly binding naringinase CLEAs onto MNPs for 10 min at room temperature, then kept it at 2–4 °C for 1–24 h. Afterwards, NM-NGase-CLEAs were separated from the supernatant by centrifuging and washing with phosphate buffer (pH 7) 3 times. For creating strong and unbroken covalent bonds, reduction of the imine bonds (C═N) of the Schiff bases formed between the glutaraldehyde ($OHC(CH_2)_3CHO$) carbonyl groups and protein (nucleophile) amino groups such as lysine residue is necessary. The rate of imine formation depends appreciably on the pH of the medium, with a maximum at low acidity (such as our research that was carried out in sodium acetate buffer at pH 5.5). In this research, ascorbic acid (1 mM in 50 mM phosphate buffer; pH 7.0) was used for the Schiff base reduction. For this purpose, 1000 μl of 1 mM ascorbic acid was added to the prepared NM-NGase-CLEAS, and the mixture was kept in the dark for 30 min at 25 °C. Excess ascorbate was then removed by adding phosphate buffer (pH 7.0) and centrifuging at 11357 ×*g* respectively.

2.2.6. Optimum glutaraldehyde concentration

Glutaraldehyde is one of the most broadly employed reagents in the biocatalysts design. The amino groups of lysine residues on the enzyme's external surface involve in cross-linking [39,40]. Cross-linker concentration also had a significant influence on the CLEAs activity. In this case, the enzymes show a lower catalytic performance (also caused by real effects on the enzyme structure) [41]. At this step, different concentrations of glutaraldehyde (1–100 mM) were employed using tert-butanol as a precipitant for CLEAs preparation under storage conditions for 4 h or 12 h, determining the optimum glutaraldehyde concentration required for stable cross-linking of naringinase.

2.2.7. Optimum holding time for CLEAs formation

The effect of holding time on the activity of the produced NM-NGase-CLEAs for optimization of the cross-linking step was performed. To determine the optimal holding time required to attain stable and firm NM-CLEAs of naringinase, the enzyme activity was measured after subjecting the enzyme to cross-linking for numerous time intervals between 1 and 24 h at 2–4 °C respectively.

2.2.8. Accessible surface area estimation of rhamnosidase and glucosidase

The crystal structure of α-L-rhamnosidase (EC 3.2.1.40) from *Bacillus sp.* (strain GL1) and β-D-glucosidase (EC 3.2.1.21) from *Aspergillus aculeatus* are resolved at a resolution of 1.9 and 1.8 Å in the monoclinic forms and have been placed in the Protein Data Bank (PDB) [42,43]. For designing of accessible surface lysine residues of naringinase that are composed of these two enzymes, by using crystallography data, the pdb format files of α-L-rhamnosidase B (2OKX) – which has a 67.3% similarity with α-L-rhamnosidase A from *Aspergillus aculeatus* by LALIGN program, for finding multiple matching subsegments in two sequences located in the Expasy website – and β-D-glucosidase (4IIB) using the GETAREA bioinformatics program for calculation of Solvent Accessible Surface Areas (with radius of the water probe 1.4 Å) of each enzyme was determined. The results are revealed in Table 1.

The GETAREA results indicated that 3 out of 14 (in α-L-rhamnosidase) and 10 out of 31 (in β-D-glucosidase) lysine residues were accessible. This information indicated that accessible surface lysine residues may be insufficient in naringinase structure for NM-NGase-CLEAs fabrication and Schiff base formation by glutaraldehyde. Thus, these data led us to the addition of lysine and/or BSA as an additive for nanomagnetic functionalization and naringinase enrichment for preparing stable CLEAs.

2.2.9. Enzyme activity and protein assay

Naringinase was estimated for its activity by measuring the amount of glucose released from the two-step hydrolysis of naringin to prunin and rhamnose by a-L-rhamnosidase and to naringenin and glucose by β-glucosidase. The glucose concentration as a reducing sugar was determined using the dinitrosalicylic acid (DNS) microassay at 575 nm (using a Perkin Elmer, Lambda 25 UV/VIS spectrophotometer in cells with 1 cm path length). The absorbance was estimated via the standard calibration curve of glucose. All experiments were repeated at least 3 times to ensure reproducibility. One unit of naringinase activity corresponds to the amount of liberated glucose as a reducing sugar per minute under standard assay conditions [44–46].

$$\text{Activity} = \mu\text{mol glucose}/\text{ min} \quad (1)$$

The protein content was assayed using Bradford microassay, from Bio-Rad protein procedure, at 595 nm (Perkin Elmer, Lambda 25 UV/VIS spectrophotometer), using a BSA calibration curve.

$$\text{Protein content} = (\text{Abs}/\text{f}) * 10\text{Df} \quad (2)$$

2.2.10. Optimum pH and temperature of free and immobilized enzyme

The optimum pH of free and immobilized naringinase was measured by incubating the reaction mixture under the various pH ranges (3–8) employing different buffers (pH 3–5, 0.1 M acetate buffer; pH 6–8, phosphate buffer) at optimum temperature [44,47]. The amount of enzyme activity was expressed as micromoles per minute for each pH value. The effect of temperature on the activity of the free and immobilized enzyme was evaluated by incubating naringinase in the buffer solution (pH 5.5) without substrate at different temperatures ranging from 40 to 80 °C for 90 min, and then the enzyme activity was measured by

Table 1
Accessible surface lysine residues in naringinase molecule.

Enzyme	PDB code	Total amino acids	Mass (Da)	Total lysine	Accessible surface lysine
α-L-rhamnosidase	2OKX	956	106,055	14	3
β-D-glucosidase	4IIB	860	93,053	31	10
Total	–	1816	199,108	45	13

Accessible Surface Area of α-L-rhamnosidase and β-D-glucosidase were estimated by GETAREA bioinformatics program for calculation of Solvent Accessible Surface Areas, with radius of the water probe 1.4 Å.

the DNS method as mentioned earlier. Enzyme activity was represented in μmol·min^{-1} at each defined temperature.

3. Results and discussion

3.1. Determination of enzyme activity and protein content

The results of this work show that optimal activity of free naringinase results after 1 min of reaction at the temperature 55 °C. However, in the case of the immobilized enzyme, this time is not changed (Fig. 1). The activity of free naringinase was 107.76 U/mg that was decreased after immobilization to 93.23 U/mg (about 13.5%). As seen from Fig. 1, although immobilized enzyme activity is reduced after immobilization, the permanence of enzyme activity increases, and it becomes more active in longer time compared to the free enzyme. The protein assay of free and immobilized enzyme were 0.133 and 0.126 (mg ml^{-1}), respectively.

3.2. Morphology of MNPs, CLEAs, and NM-NGase-CLEAs

The morphology and size of the obtained MNPs were studied using FE-SEM (Fig. 2). As shown in Fig. 2, the characteristics of the produced MNPs, NGase-CLEAs, and NM-NGase-CLEAs indicated that nanomagnetites were observed to have semi-spherical and spherical morphology and uniformly distributed in the acquired water-based MNPs with a mean diameter of about 50–60 nm (Fig. 2A). CLEAs that were formed from enzyme aggregates are composed of two enzymes (α-L-rhamnosidase and β-D-glucosidase) and have two different shapes and sizes, contain larger cubic particles and semi-cubic rods together with smaller spherical and semi-spherical particles with various particle sizes between 0.5-20 μm respectively (Fig. 2B, C, D). Probably, these two different shapes and sizes are attributed to the differences in mass and conformation of these two enzymes [α-L-rhamnosidase with 956 amino acids and 106,055 mass (Da) and β-D-glucosidase with 860 amino acids and 93,053 mass (Da)].

NM-NGase-CLEAs revealed a morphology of non-uniform, semi-pyramid and semi-cubic rods, with a mean diameter of about 10–100 nm (Fig. 2E, F).

The presence of the MNPs and NM-NGase-CLEAs (immobilized enzyme on Fe_3O_4) was confirmed by exploiting EDX, which determined the elemental composition of these particles (see Table 2).

As Table 2 shows, the maximum amount of iron and oxygen elements are available in Fe3O4, non-magnetic CLEAs have a higher carbon and nitrogen content, NM-Ngase-CLEAs have a higher iron content compared to the non-NM-CLEAs, and it contains more carbon and nitrogen elements than Fe3o4; hence, the existence of the MNPs in the NM-NGase-CLEAs was confirmed by means of EDX, which determined the elemental composition of naringinase CLEAS, with and without magnetic nanoparticles.

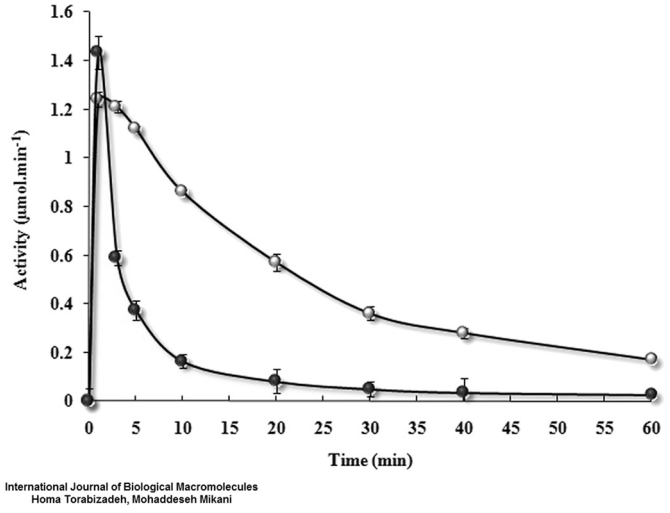

Fig. 1. Enzyme activity profile of free and immobilized naringinase. Free enzyme (●), immobilized enzyme (○).

3.3. Particle size, PDI, and zeta-potential of fabricated NM-NGase-CLEAS

The particle size, PDI, and Ζ-potential of MNPs and NM-NGase-CLEAs were determined by the DLS method. The resulted data revealed that the nanomagnetite particle size mostly was around 81.9–96.5 nm (Fig. 3A) and that after enzyme immobilization and NM-NGase-CLEAS formation, this particle size was reduced to around 13.2–15.3 nm respectively (Fig. 3B).

The DLS of MNPs and NM-NGase-CLEAs confirmed the FE-SEM image outcomes, but the particle diameter using the DLS measurement was a little smaller than the results from the FE-SEM image. This difference was possibly owing to the shrinkage caused by the cast-drying process as well as the vacuum environment in the FE-SEM image. Based on the results obtained from the DLS method, the PDI of Fe_3O_4 was equal to 0.238 and the NM-NGase-CLEAs–related PDI was 0.177, respectively. These results implied that after functionalization of Fe_3O_4 surface with lysine amino acid and immobilization of naringinase and formation of NM-NGase-CLEAs, the PDI index reduces, which can be attributed to binding of the magnetite to protein nanoparticles and increasing of hydrophilicity, thereby improving the stability of produced nanoparticles. Moreover, the Ζ-potential of −28 mV also confirms this claim. Since, the DLS test is carried out in a liquid environment, the actual dispersity of nanoparticles can be estimated more accurately than the SEM test, which has been tested for dry and lyophilized samples.

3.4. FTIR results

The FTIR analysis of Fe_3O_4 and NM-NGase-CLEAs were carried out from 400 to 4000 cm^{-1} as revealed in Fig. 4A. As shown in Fig. 4A, the spectrum of Fe_3O_4 before enzyme immobilization indicated Fe—O stretching vibration at 600 cm^{-1}, the adsorbed water molecules stretching at 1621 cm^{-1} and an intense OH band around 3400 cm^{-1}. The OH band corresponded to the stretching vibrations of Fe-OH groups attached on the Fe_3O_4 surface and can also be pointed to the remaining water that was not omitted from the nanomagnetite surface. The NM-NGase-CLEAs peak at 602 cm^{-1} indicated Fe—O stretching vibration, and another peak is at 1047 cm^{-1}, which is corresponding to the reduced Schiff base (C—N) group (1020–1250 cm^{-1}) – which could be attributed to reduction of the Schiff base (-C=N) bond that is formed by the reaction of NH_2 end groups with glutaraldehyde by ascorbic acid – as well as the peak at 1086 cm^{-1} is attributed to the stretching vibration mode of C—O group. Other peaks at 1384 cm^{-1}, 1637 cm^{-1}, and 3418 cm^{-1} were attributed to the stretching vibration mode of CH_3, NH_2 and/or C=O amide, N—H and/or alcohol OH bonds, respectively. The significant peak of enzyme at 1637 cm^{-1} corresponded to the vibrations of the backbone C=O, belonging to the vibration of amide groups in the FTIR spectrum.

3.5. UV–vis spectra of naringinase, naringin, Fe_3O_4, and NM-NGase-CLEAs

The UV analysis of naringinase, naringin, nanomagnetites, lysine functionalized Fe_3O_4, and NM-NGase-CLEAs were performed at 200–600 nm (Fig. 4B and C). Naringinase possessed two main λ_{max} in the UV region: one between 215–225 nm, where the peptide bonds absorbed, and the second at 260–270 nm (Fig. 4B), due to light absorption by aromatic amino acids [48,49].

Naringin exhibited one main λ_{max} in the UV region at 250 nm (Fig. 4B). Comparison of UV spectra of Fe_3O_4 and lysine-functionalized Fe_3O_4 implied that after nanomagnetite functionalization, one new peak is formed at 440 nm, which can be attributed to the binding of

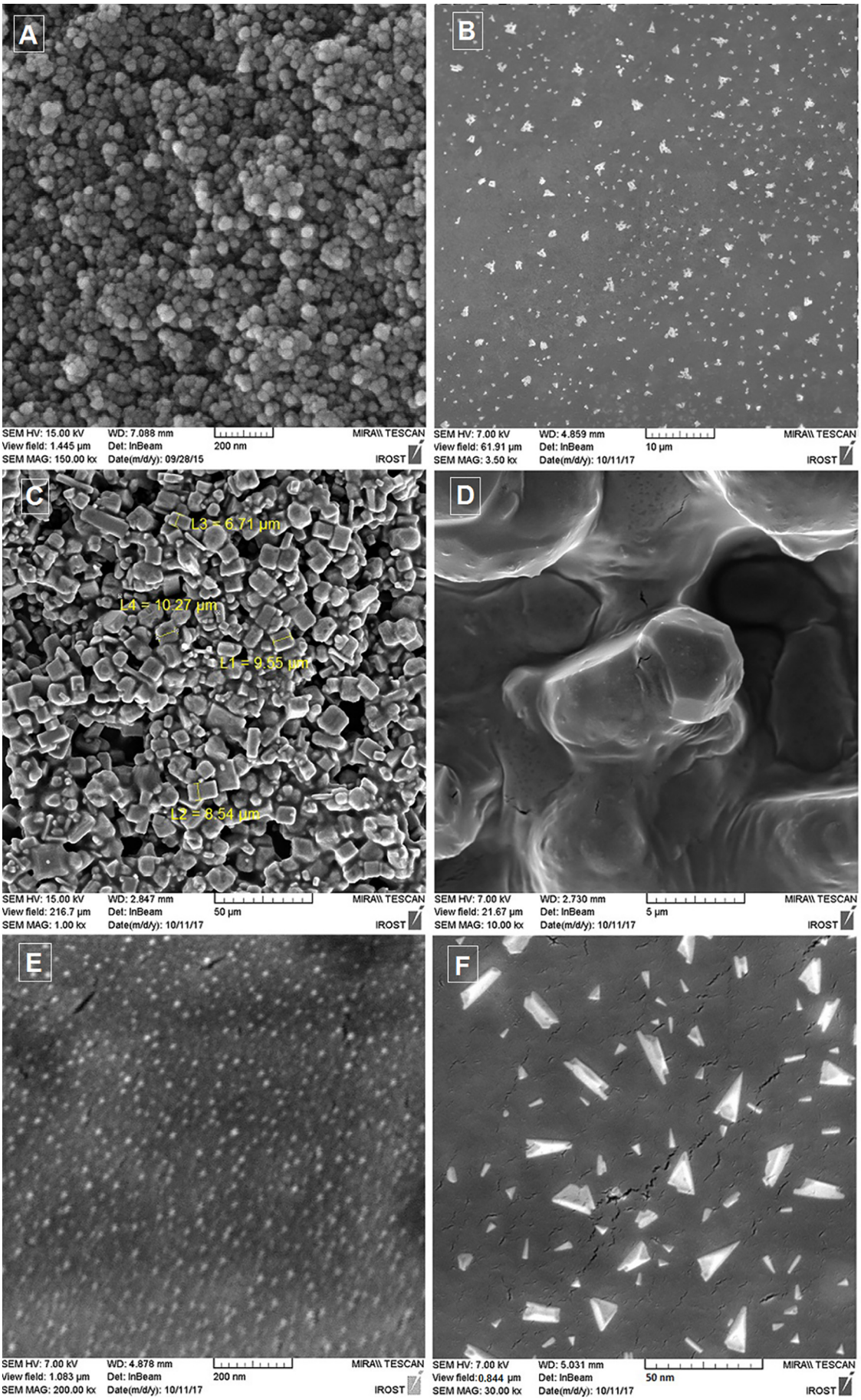

Fig. 2. Scanning electron microscopy images of (A) magnetic nanoparticles, (B, C, D) naringinase CLEAs with different magnifications, (E, F) NM-Ngase-CLEAs with different magnifications.

Table 2
EDX for elemental composition of Fe3O4, CLEAs, NM-NGase-CLEAs.

Elements (W%)	Fe_3O_4	CLEAs	NM-NGase-CLEAs
C	15.98	34.19	35.05
N	12.21	28.60	28.23
O	70.84	37.20	36.08
Fe	0.97	0.01	0.64
Total	100	100	100

lysine to magnetic nanoparticles. The results revealed that after enzyme immobilization and addition of lysine/naringinase ratio equal to 10, during nanomagnetic CLEAs fabrication, the peptide bonds and aromatic amino acids are reinforced, and the protein structure is preserved during NM-NGase-CLEAs preparation (Fig. 4C).

3.6. Effect of precipitating agents

Protein molecules are able to aggregate as accumulative molecular structures without disrupting the original protein three-dimensional structures by exposure to an environment with high ionic strength (salts), non-ionic polymers, or organic solvents. The precipitation step extremely affects the activity and stability of fabricated CLEAs. Accordingly, selection of the best precipitant in enzyme aggregation process is very important and it depends on the nature of the enzyme, the mode and duration of the precipitation step, and the temperature and pH used in the aggregation process [26]. In this step, acetone, acetonitrile, ethanol, isopropanol, tert-butanol and saturated ammonium sulfate solution were applied as precipitants; then, the enzyme activity assay was carried out for all aggregates prior to cross-linking process. The results are shown in Fig. 5A. The maximum activity in the precipitation step was displayed by using tert-butanol. In contrast, the lowest activity value was related to the naringinase aggregate which was prepared in saturated ammonium sulfate under the same conditions. The activity of aggregates in tert-butanol increased 13.97% and 75.4% compared to the free enzyme and produced aggregates in saturated ammonium sulphate, respectively. In fact, tert-butanol that is a miscible polar organic solvent decreases the dielectric constant of water molecules (dielectric constant (ε) for water molecules is 78.3 and for tert-butanol is 12.5) around the enzyme molecules and progressively displaces water from the protein surface. With smaller hydration layers, enzyme molecules can aggregate by attractive electrostatic and dipole forces [50]. The control showed the activity of free enzyme with no addition of precipitant, at pH 5.5, which corresponds to the conditions usually employed in hydrolysis reactions. Since tert-butanol provided the best overall outcomes, it was chosen as a suitable precipitant for CLEAs preparation in further experiments.

3.7. Effect of the BSA and lysine concentrations

Since the protein content in naringinase was low (0.133 $mg \cdot ml^{-1}$), as well as the accessible surface area determination of naringinase implied that 13 lysine residues out of 45 are accessible for reaction by glutaraldehyde, therefore, it may be insufficient that adding BSA (with 118 lysine residues in its structure) for enrichment of the enzyme structure in aggregation and cross-linking processes was necessary. Moreover, addition of an amino acid with reactive ε-amino groups like lysine during enzyme aggregation in CLEAs could overcome this problem. For this purpose, the effect of BSA and lysine on the activity of the aggregated naringinase after cross-linking was studied. Subsequent addition of glutaraldehyde to this concentrated protein solution in the presence of adequate free amino groups facilitates the production of insoluble and active CLEA particles through efficient cross-linking. The effect of lysine/enzyme and BSA/enzyme ratios on the activity of CLEAs was evaluated. Various lysine and/or BSA/naringinase ratios (2.5, 5, 10, 20, and 40) were prepared during the aggregation process, and the resultant CLEAs activity was determined as mentioned previously. The results revealed that lysine addition to naringinase in the ratio of 10:1 is more efficient than BSA because it leads to the maximal activity (1.36 times greater than BSA/enzyme activity at the same ratio) for prepared CLEAs compared to the free enzyme (Fig. 5B).

The ratios less than optimal value resulted in unstable CLEAs structure, thus leaching and losing of the enzyme during the washing process occurred. In contrast, high ratios than optimal value lead to inhibit the essential cross-linking of naringinase molecules, caused by competition between the free amino groups of lysine and those of the naringinase [51]. Based on these results, a lysine to naringinase ratio equal to 10:1 was employed in all further experiments.

3.8. Effect of glutaraldehyde concentration and holding time

The effect of the cross-linker amount (1–100 mM) on the resultant CLEAs activity was studied for the cross-linking step optimization. The results shown in Fig. 5C. The highest enzyme activity of CLEAs was observed when a 10 mM glutaraldehyde concentration was applied. As a result, the concentration of glutaraldehyde is significant in the process and can influence the CLEAs performance.

Poor strength of cross-linked NM-naringinase may occur when low concentration of glutaric dialdehyde (<10 mM) was used. The CLEAs activity was lower based on insufficient cross-linking, which lead to

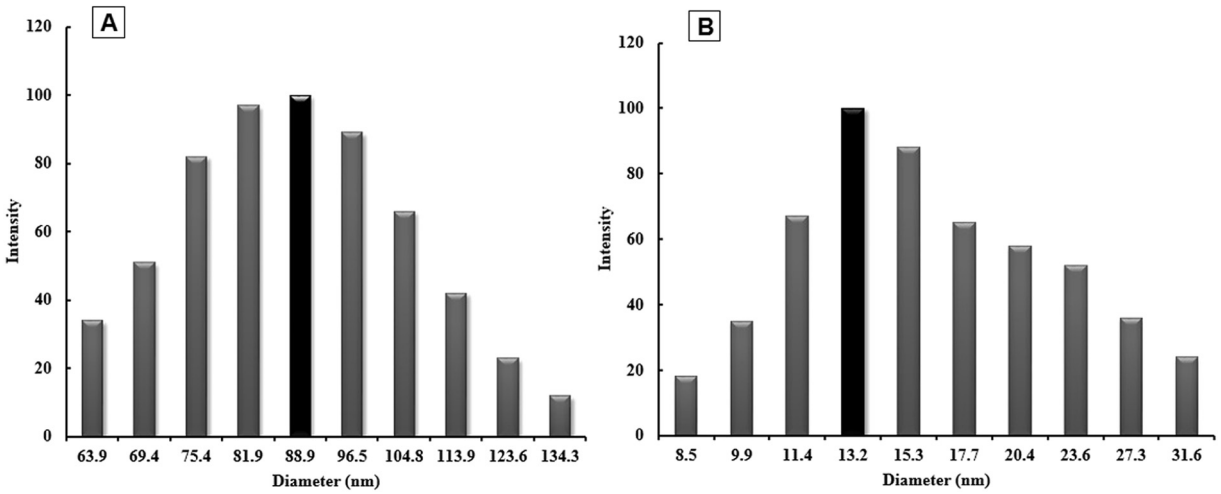

Fig. 3. Particle size distribution of magnetic nanoparticles and NM-NGase-CLEAs by DLS methods. (A) magnetic nanoparticles, (B) NM-NGase-CLEAs.

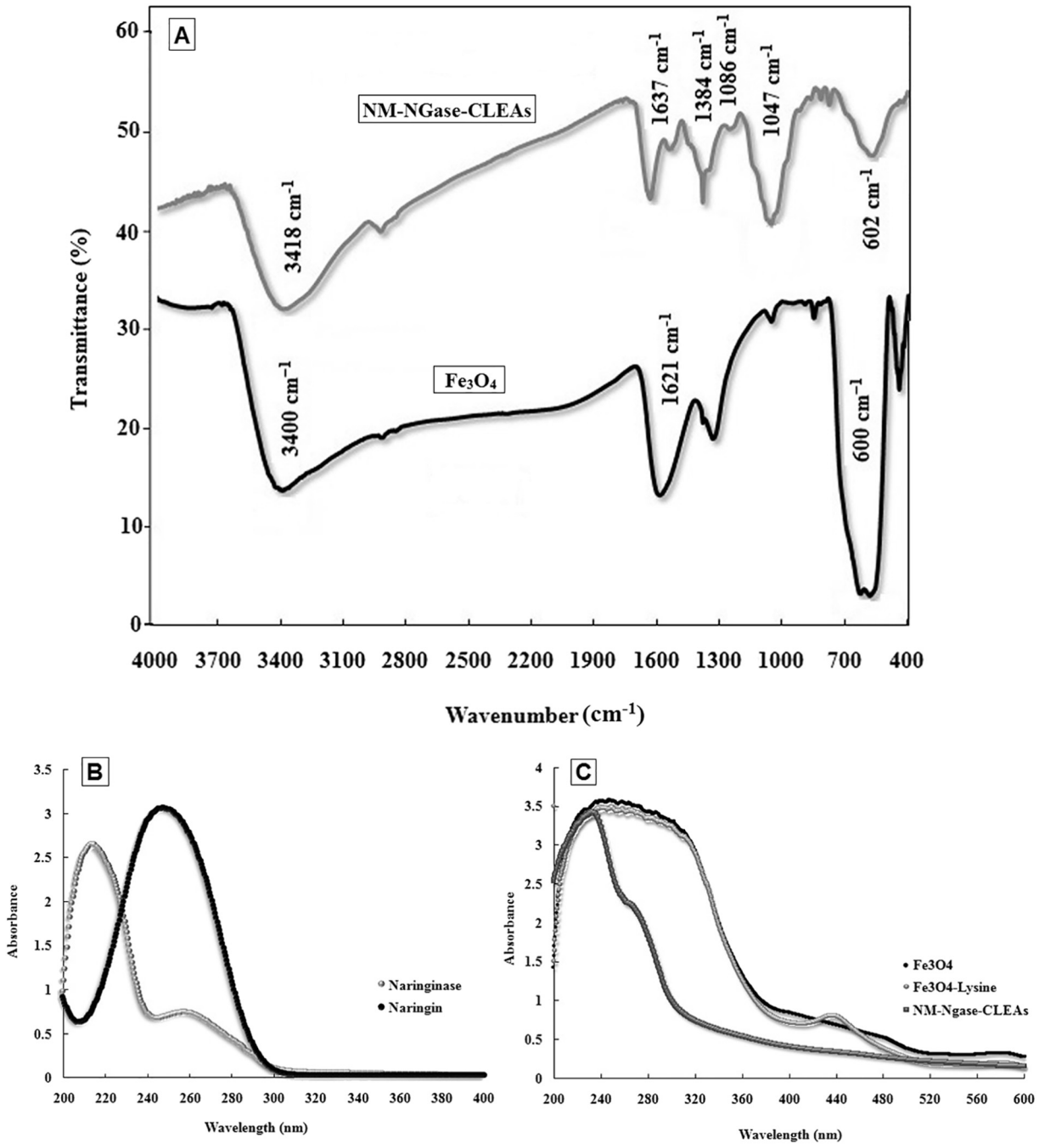

Fig. 4. FTIR spectra at 4000–400 cm^{-1} of (A) magnetic nanoparticles compared to NM-NGase-CLEAs. UV–Vis spectra of (B) naringin and naringinase at 200–400 nm and (C) Fe_3O_4, Fe_3O_4-Lysine, and NM-Ngase-CLEAs at 200–600 nm.

unstable aggregation. In the same way, at high glutaraldehyde concentrations (>10 mM), excessive cross-linking restrains the enzyme's flexibility and reduces mass transfer, leading to a decrease in enzyme activity.

The results of the CLEAs holding time (1–24 h) implied that maximum enzyme activity achieved after 4 h, holding CLEAs at 2–4 °C. The enzyme activity significantly improved by increasing the holding time until 4 h, even though cross-linking for longer time periods, >3 h, revealed lower enzyme activity (Fig. 5D).

3.9. Temperature and pH effects

The effect of pH on both free naringinase and CLEAs activities was determined in the pH ranges of 5–9 for 90 min at 50 °C respectively. The pH optimum of free and immobilized enzymes for naringin hydrolysis was found to be 5.5. Therefore, based on the resulted data, there were no significant changes in the pH optimum of the enzyme after NM-NGase-CLEAs preparation (Fig. 6A).

The effect of temperature on the activity of free and immobilized naringinase was also determined. The samples were exposed to different temperatures ranging from 40 to 80 °C, at a pH of 5.5 for 90 min. The results implied that the temperature optimum of immobilized enzyme is shifted upward by 10 °C since the NM-NGase-CLEAs reached their maximum activity at 60 °C, while the maximum activity of free naringinase was obtained at 50 °C (Fig. 6B). This demonstrates that the immobilization significantly raised the stability of naringinase at higher temperatures. As shown in Fig. 6B, the immobilized naringinase displayed a

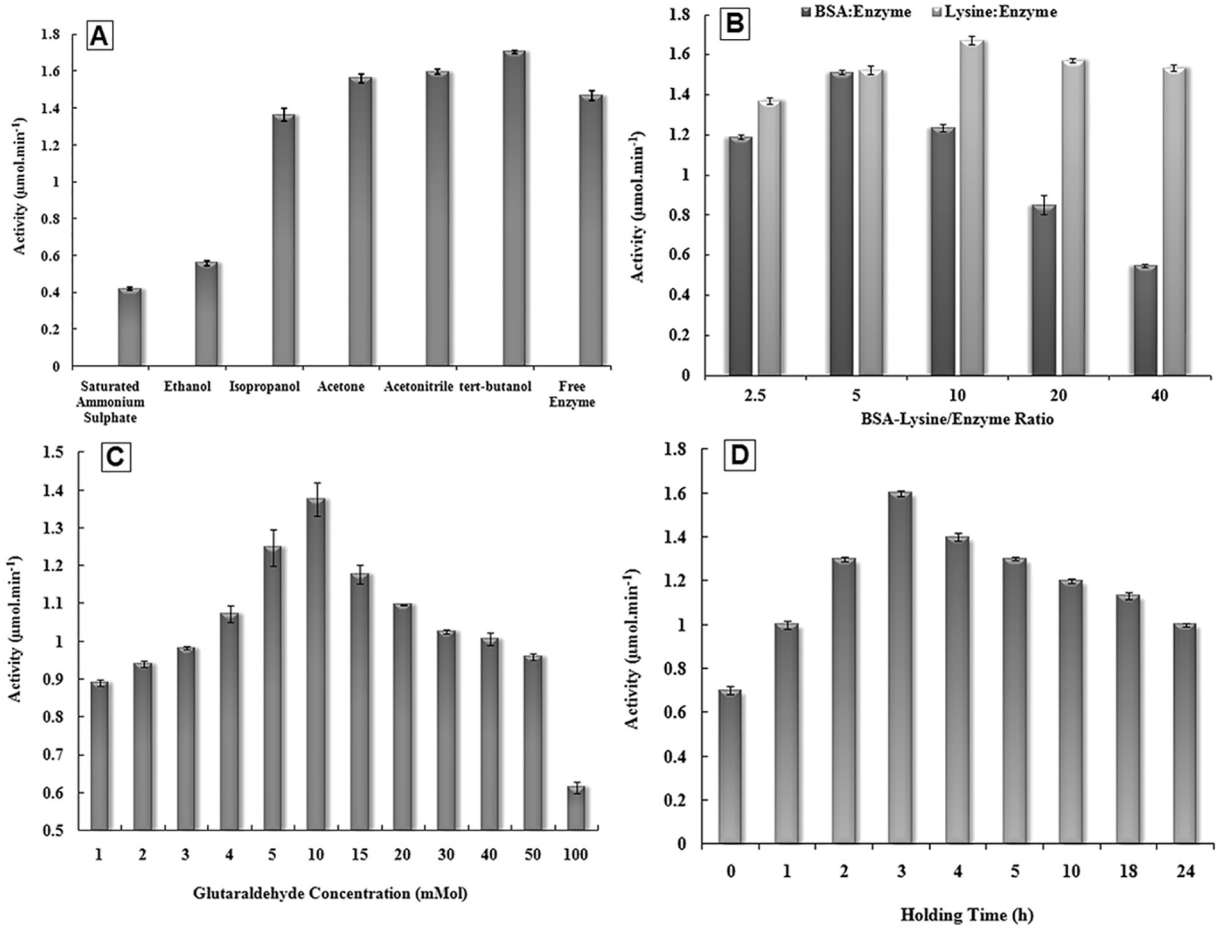

Fig. 5. Effect of (A) various precipitating agents on the activity of naringinase aggregates compared to free enzyme, (B) various BSA and lysine to naringinase ratios, (C) different glutaraldehyde concentrations, (D) various CLEAs holding time on the enzyme activity.

considerable increment in thermostability as compared with its free one [52]. This increment in optimum temperature and thermal stability of NM-NGase-CLEAs could be due to the formation of covalent bonds during cross-linking process and limitation in free movement of enzyme molecules – as a result, preservation of amino acids at the active site of the enzyme. This feature will lead the NM-CLEAs to increase thermostability of the naringinase within a wider temperature range that will have a decisive role in industrial applications [53] of this enzyme, such as debittering of citrus juices as well as prevention of microbial growth [54–56].

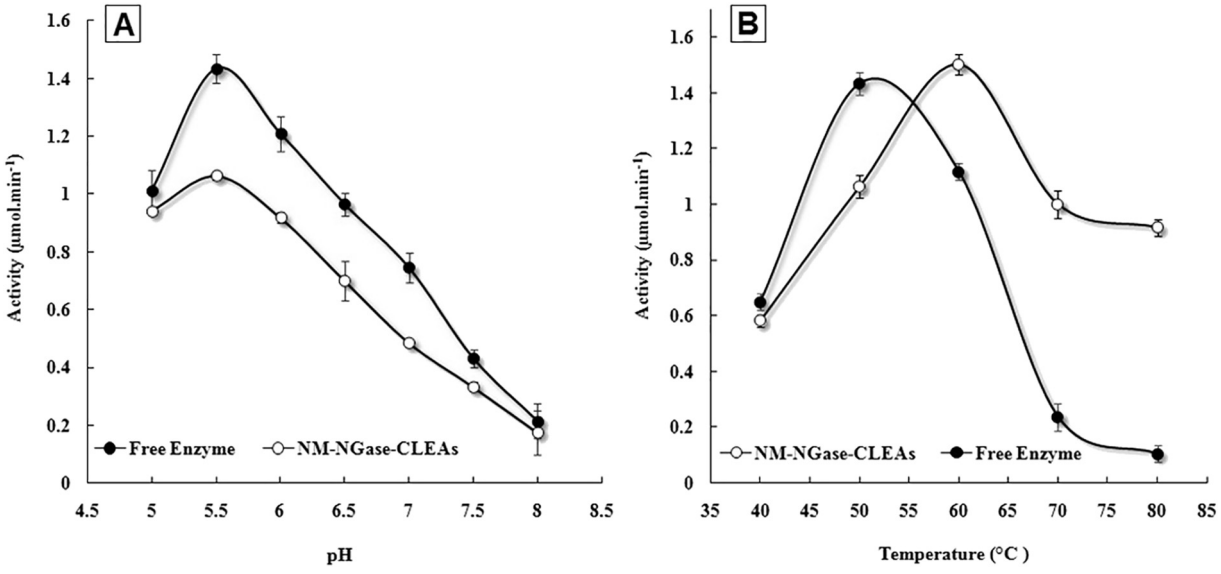

Fig. 6. Effect of pH and temperature on the initial enzymatic activity of free and immobilized enzyme. Free (●) and immobilized (○) enzyme. (A) the effect of pH, (B) the effect of temperature.

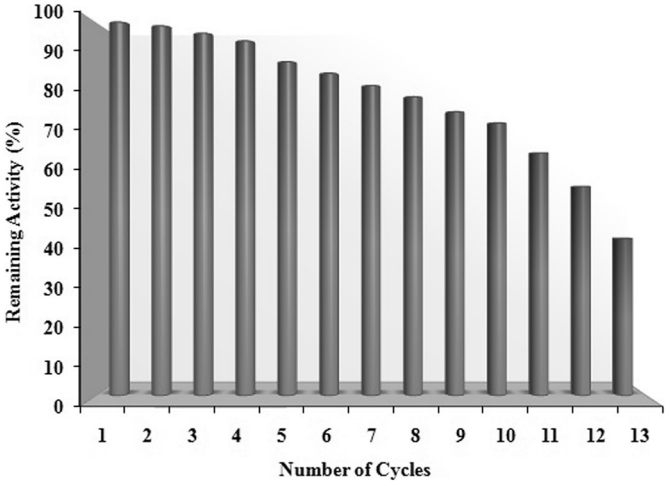

Fig. 7. Effect of the enzyme reuses on the activity of NM-NGase-CLEAs during naringin hydrolysis at pH 5.5 and 60 °C for 90 min. Each treatment was performed in triplicate.

3.10. Reusability of NM-CLEAs

Enzyme immobilization supplies an interesting opportunity for multiple use of the same biocatalyst. The main purpose for the synthesis of NM-CLEAs is to finally design suitable reusable immobilized enzymes that can be easily eliminated from the reaction medium during downstream processing, with maximum recovery of enzymatic activity for reducing production costs of the industrial processes. To this end, the efficiency of reusing naringinase NM-CLEAs was estimated up to 13 cycles (Fig. 7). The activity of naringinase NM-CLEAs kept 73% of its original activity after 10 cycles, which proposes strong operational stability.

4. Conclusions

Nanomagnetic cross-linked enzyme aggregates of naringinase from *Aspergillus aculeatus* was fabricated as a new efficient nanobiocatalyst for naringin hydrolysis. The main features of NM-NGase-CLEAs are: mean particle size = 13.2–15.3 nm, PDI = 0.177, Ζ-potential = −28 mV, high thermostability over a wide range of pH and temperature. Moreover, NM-CLEAs of naringinase have remarkable high reusability over 10 cycles of hydrolysis. Adding ascorbic acid to the NM-Ngase-CLEAs for Schiff base reduction of formed bonds enhanced its strength. That's why the NM-NGase-CLEAs could be introduced as an effective nanobiocatalyst for industrial applications such as the debittering process of citrus juices.

Acknowledgments

The authors are grateful for the financial support provided by the Iranian Research Organization for Science and Technology (IROST) of Iran (grant 2016/1010295027).

Funding

This work was supported by the Iranian Research Organization for Science and Technology of Iran, Tehran, Iran [grant 2016/1010295027].

References

[1] M.E. Khosroshahi, L. Ghazanfari, Synthesis of three-layered magnetic based nanostructure for clinical application, Int. J. Nanosci. Nanotechnol. 7 (2011) 57–64.
[2] G.E.A. Awad, A.A. Aty, A.N. Shehata, M.E. Hassan, M.M. Elnashar, Covalent immobilization of microbial naringinase using novel thermally stable biopolymer for hydrolysis of naringin, 3 Biotech. 6 (2016) 14–24, https://doi.org/10.1007/s13205-015-0338-x.
[3] M.D. Busto, V. Meza, N. Ortega, M. Perez-Mateos, Immobilization of naringinase from *Aspergillus niger* CECT 2088 in poly (vinyl alcohol) cryogels for the debittering of juices, Food Chem. 104 (2007) 1177–1182, https://doi.org/10.1016/j.foodchem.2007.01.033.
[4] A. Alvarenga, M.J. Amoroso, A. Illanes, G.R. Castro, Crosslinked alpha-L-rhamnosidase aggregates with potential application in food industry, Eur. Food Res. Technol. 238 (2014) 797–801, https://doi.org/10.1007/s00217-014-2157-4.
[5] Q. Liu, L. Lu, M. Xiao, Cell surface engineering of α-L-rhamnosidase for naringin hydrolysis, Bioresour. Technol. 123 (2012) 144–149, https://doi.org/10.1016/j.biortech.2012.05.083.
[6] M. Misson, H. Zhang, B. Jin, Nanobiocatalyst advancements and bioprocessing applications, J. R. Soc. Interface 12 (2014), 20140891. https://doi.org/10.1098/rsif.2014.0891.
[7] Y. Jiang, C. Cui, Y. Huang, X. Zhang, J. Gao, Enzyme-based inverse opals: a facile and promising platform for fabrication of biocatalysts, Chem. Commun. 50 (2014) 5490–5493, https://doi.org/10.1039/C4CC01721H.
[8] J. Gao, W. Kong, L. Zhou, Y. He, L. Ma, Y. Wang, L. Yin, Y. Jiang, Monodisperse core-shell magnetic organosilica nanoflowers with radial wrinkle for lipase immobilization, Chem. Eng. J. 309 (2017) 70–79, https://doi.org/10.1016/j.cej.2016.10.021.
[9] Y. Jiang, L. Shi, Y. Huang, J. Gao, X. Zhang, L. Zhou, Preparation of robust biocatalyst based on cross-linked enzyme aggregates entrapped in three-dimensionally ordered macroporous silica, ACS Appl. Mater. Interfaces 6 (2014) 2622–2628, https://doi.org/10.1021/am405104b.
[10] Á. Cruz-Izquierdo, E.A. Picó, C. López, J.L. Serra, M.J. Llama, Magnetic cross-linked enzyme aggregates (mCLEAs) of *Candida antarctica* lipase: an efficient and stable biocatalyst for biodiesel synthesis, PLoS One 9 (2014), e115202. https://doi.org/10.1371/journal.pone.0115202.
[11] J. Cui, S. Jia, L. Liang, Y. Zhao, Y. Feng, Mesoporous CLEAs-silica composite microparticles with high activity and enhanced stability, Sci. Rep. 5 (2015) 14203, https://doi.org/10.1038/srep14203.
[12] S.S. Singh, A.J. Young, S. Woo-Ri, K.J. Ho, L. Lyon, D. Maisie, T. John, H. Janet, K.S. Yong, M. Jiho, K. Yang-Hoon, Immobilization of cross-linked cutinase aggregates onto magnetic beads for degradation of polycaprolactone, J. Nanosci. Nanotechnol. 17 (2017) 9306–9311, https://doi.org/10.1166/jnn.2017.13904.
[13] Y.V. Samoylova, K.N. Sorokina, A.V. Piligaev, V.N. Parmon, Preparation of stable cross-linked enzyme aggregates (CLEAs) of a *Ureibacillus thermosphaericus* esterase for application in malathion removal from wastewater, Catalysts 8 (2018) 154, https://doi.org/10.3390/catal8040154.
[14] A.B. Martínez-Moñino, R. Zapata-Pérez, A.G. García-Saura, J. Cabanes, Á. Sánchez-Ferrer, A new cross-linked enzyme aggregate biocatalyst for NAD^+-booster production, RSC Adv. 7 (2017) 14272–14278, https://doi.org/10.1039/C7RA00505A.
[15] M.M. Nikje, L. Sarchami, L. Rahmani, Fabrication of 2-chloropyridine functionalized Fe_3O_4/amino-silane core–shell nanoparticles, Int. J. Nanosci. Nanotechnol. 11 (2015) 39–44.
[16] S. Kayal, R.V. Ramanujan, Anti-cancer drug loaded iron- gold core-shell nanoparticles (Fe@Au) for magnetic drug targeting, J. Nanosci. Nanotechnol. 10 (2010) 5527–5539, https://doi.org/10.1166/jnn.2010.2461.
[17] H.Y. Park, M.J. Schadt, L. Wang, I.S. Lim, P.N. Njoki, S.H. Kim, M.Y. Jang, J. Luo, C.J. Zhong, Fabrication of magnetic core@shell Fe oxide@Au nanoparticles for interfacial bioactivity and bio-separation, Langmuir 23 (2007) 9050–9056, https://doi.org/10.1021/la701305f.
[18] M.E. Khosroshahi, L. Ghazanfari, Preparation and characterization of silica-coated iron-oxide bionanoparticles under N_2 gas, Physica E Low Dimens. Syst. Nanostruct. 42 (2010) 1824–1829, https://doi.org/10.1016/j.physe.2010.01.042.
[19] C.G. Netto, H.E. Toma, L.H. Andrade, Superparamagnetic nanoparticles as versatile and supporting materials for enzymes, J. Mol. Catal. B Enzym. 85 (2013) 71–92, https://doi.org/10.1016/j.molcatb.2012.08.010.
[20] M.L. Verma, M. Naebe, C.J. Barrow, M. Puri, Enzyme immobilisation on amino-functionalised multi-walled carbon nanotubes: structural and biocatalytic characterization, PLoS One 8 (2013), e73642. https://doi.org/10.1371/journal.pone.0073642.
[21] B.L.A.P. Devi, Z. Guo, X. Xu, Characterization of cross-linked lipase aggregates, J. Am. Oil Chem. Soc. 86 (2009) 637–642, https://doi.org/10.1007/s11746-009-1401-8.
[22] F. Contesini, J. Figueira, H. Kawaguti, P. Fernandes, P. Carvalho, Potential applications of carbohydrases immobilization in the food industry, Int. J. Mol. Sci. 14 (2013) 1335–1369, https://doi.org/10.3390/ijms14011335.
[23] R. Sheldon, S. Van Pelt, Enzyme immobilization in biocatalysis: why, what and how, Chem. Soc. Rev. 42 (2013) 6223–6235, https://doi.org/10.1039/C3CS60075K.
[24] R. Sheldon, Characteristic features and biotechnological applications of cross-linked enzyme aggregates (CLEAs), Appl. Microbiol. Biotechnol. 92 (2011) 467–477, https://doi.org/10.1007/s00253-011-3554-2.
[25] R. Sheldon, Cross-linked enzyme aggregates (CLEAs): stable and recyclable biocatalysts, Biochem. Soc. Trans. 35 (2007) 1583–1587, https://doi.org/10.1042/BST0351583.
[26] M.H.L. Ribeiro, M. Rabaça, Cross-linked enzyme aggregates of naringinase: novel biocatalysts for naringin hydrolysis, Enzym. Res. 2011 (2011) 851272, https://doi.org/10.4061/2011/851272.
[27] A. Cruz-Izquierdo, E.A. Picó, Z. Anton-Helas, C.G. Boeriu, M. Llama, Lipase immobilization to magnetic nanoparticles: methods, properties and applications for biobased products, New Biotechnol. 29 (2012) S100–S101.
[28] H. Torabizadeh, M. Habibi Rezaei, M. Safari, A.A. Moosavi- Movahedi, H. Razavi, Semi-rational chemical modification of endoinulinase by pyridoxal 5′-phosphate and ascorbic acid, J. Mol. Catal. B Enzym. 62 (2010) 257–264, https://doi.org/10.1016/j.molcatb.2009.10.007.
[29] M. Tudorache, A. Nae, S. Coman, V. Parvulescu, Strategy of cross-linked enzyme aggregates onto magnetic particles adapted to the green design of biocatalytic

synthesis of glycerol carbonate, RSC Adv. 3 (2013) 4052–4058, https://doi.org/10.1039/C3RA23222K.
[30] J.D. Cui, L.L. Cui, S.P. Zhang, Y.F. Zhang, Z.G. Su, G.H. Ma, Hybrid magnetic cross-linked enzyme aggregates of phenylalanine ammonia lyase from *Rhodotorula glutinis*, PLoS One 9 (2014), e97221. https://doi.org/10.1371/journal.pone.0097221.
[31] A. Krishna Sailaja, P. Amareshwar, P. Chakravarty, Different techniques used for the preparation of nanoparticles using natural polymers and their application, Int J Pharm Pharm Sci 3 (2011) 45–50.
[32] M. Mascolo, Y. Pei, T. Ring, Room temperature Co-precipitation synthesis of magnetite nanoparticles in a large pH window with different bases, Materials (Basel) 6 (2013) 5549–5567, https://doi.org/10.3390/ma6125549.
[33] N. Kandpal, N. Sah, R. Loshali, R. Joshi, J. Prasad, Coprecipitation method of synthesis and characterization of iron oxide nanoparticles, J. Sci. Ind. Res. 73 (2014) 87–90.
[34] H. Yamaguchi, M. Miyazaki, Y. Asanomi, H. Maeda, Poly-lysine supported cross-linked enzyme aggregates with efficient enzymatic activity and high operational stability, Catal. Sci. Technol. 1 (2011) 1256–1261, https://doi.org/10.1039/c1cy00084e.
[35] A.K. Gupta, M. Gupta, Synthesis and surface engineering of iron oxide nanoparticles for biomedical applications, Biomaterials 26 (2005) 3995–4021, https://doi.org/10.1016/j.biomaterials.2004.10.012.
[36] L. Zhanfeng, Q. Linhui, Z. Shuangling, W. Hongyan, C. Xuejun, Synthesis and characterization of monodisperse magnetic Fe_3O_4@BSA core–shell nanoparticles, Colloids Surf. A Physicochem. Eng. Asp. 436 (2013) 1145–1151, https://doi.org/10.1016/j.colsurfa.2013.08.044.
[37] J.L. Viota, F.J. Arroyo, A.V. Delgado, J. Horno, Electrokinetic characterization of magnetite nanoparticles functionalized with amino acids, J. Colloid Interface Sci. 344 (2010) 144–149, https://doi.org/10.1016/j.jcis.2009.11.061.
[38] I. Antal, M. Koneracka, M. Kubovcikova, V. Zavisova, I. Khmara, D. Lucanska, L. Jelenska, I. Vidlickova, M. Zatovicova, S. Pastorekova, N. Bugarova, M. Micusik, M. Omastova, P. Kopcansky, D,L-lysine functionalized Fe_3O_4 nanoparticles for detection of cancer cells, Colloids Surf. B: Biointerfaces 163 (2018) 236–245, https://doi.org/10.1016/j.colsurfb.2017.12.022.
[39] O. Barbosa, C. Ortiz, A. Berenguer-Murcia, R. Torres, R.C. Rodrigues, R. Fernandez-Lafuente, Strategies for the one-step immobilization-purification of enzymes as industrial biocatalysts, Biotechnol. Adv. 33 (2015) 435–456, https://doi.org/10.1016/j.biotechadv.2015.03.006.
[40] E.T. Hwang, M.B. Gu, Enzyme stabilization by nano/microsized hybrid materials, Eng. Life Sci. 13 (2012) 49–61, https://doi.org/10.1002/elsc.201100225.
[41] R. Rodrigues, C. Ortiz, A. Berenguer-Murcia, R. Torres, R. Fernández-Lafuente, Modifying enzyme activity and selectivity by immobilization, Chem. Soc. Rev. 42 (2013) 6290–6307, https://doi.org/10.1039/c2cs35231a.
[42] Z. Cui, Y. Maruyama, B. Mikami, W. Hashimoto, K. Murata, Crystal structure of glycoside hydrolase family 78 alpha-L-Rhamnosidase from Bacillus sp. GL1, J. Mol. Biol. 374 (2007) 384–398, https://doi.org/10.1016/j.jmb.2007.09.003.
[43] K. Suzuki, J. Sumitani, Y.W. Nam, T. Nishimaki, S. Tani, T. Wakagi, T. Kawaguchi, S. Fushinobu, Crystal structures of glycoside hydrolase family 3 beta-glucosidase 1 from *Aspergillus aculeatus*, Biochem. J. 452 (2013) 211–221, https://doi.org/10.1042/BJ20130054.
[44] H. Torabizadeh, M. Tavakoli, M. Safari, Immobilization of thermostable α-amylase from *bacillus licheniformis* by cross-linked enzyme aggregates method using calcium and sodium ions as additives, J. Mol. Catal. B Enzym. 108 (2014) 13–20, https://doi.org/10.1016/j.molcatb.2014.06.005.
[45] J. Missau, A. Scheid, E. Foletto, S. Jahn, M. Mazutti, R. Kuhn, Immobilization of commercial inulinase on alginate-chitosan beads, Sustainable Chem. Processes 2 (2014) 13–19.
[46] A. Richetti, C. Munaretto, L. Lerin, L. Batistella, J. Oliveira, R. Dallago, V. Astolfi, M. Diluccio, Immobilization of inulinase from *Kluyveromyces marxianus* NRRL Y-7571 using modified sodium alginate beads, Bioprocess Biosyst. Eng. 35 (2012) 383–388, https://doi.org/10.1007/s00449-011-0576-1.
[47] T. Yewale, R.S. Singhal, A.A. Vaidya, Immobilization of inulinase from *Aspergillus niger* NCIM 945 on chitosan and its application in continuous inulin hydrolysis, Biocatal. Agric. Biotechnol. 2 (2013) 96–101.
[48] D.A. Skoog, F.J. Holler, S.R. Crontch, Principles of instrumental analysis, sixth ed. Thomson Brooks/Cole, Canada, 2007.
[49] P. Singh, P.K. Gill, Production of inulinases: recent advances, Food Technol. Biotechnol. 44 (2006) 151–162.
[50] N. Ramachandran, E.S. Hamborg, G.F. Versteeg, The effect of aqueous alcohols (methanol, t-butanol) and sulfolane on the dissociation constants and thermodynamic properties of alkanolamines, Fluid Phase Equilib. 360 (2013) 36–43, https://doi.org/10.1016/j.fluid.2013.08.040.
[51] S. Shah, A. Sharma, M.N. Gupta, Preparation of cross-linked enzyme aggregates by using bovine serum albumin as a proteic feeder, Anal. Biochem. 351 (2006) 207–213, https://doi.org/10.1016/j.ab.2006.01.028.
[52] A. Homaei, R. Etemadipour, Improving the activity and stability of actinidin by immobilization on gold nanorods, Int. J. Biol. Macromol. 72 (2015) 1176–1181, https://doi.org/10.1016/j.ijbiomac.2014.10.029.
[53] M. Vršanská, S. Vob˙erková, A.M. Jiménez Jiménez, V. Strmiska, V. Adam, Preparation and optimisation of cross-linked enzyme aggregates using native isolate white rot Fungi *Trametes versicolor* and *Fomes fomentarius* for the decolourisation of synthetic dyes, Int. J. Environ. Res. Public Health 23 (2018) 1–15, https://doi.org/10.3390/ijerph15010023.
[54] Q. Nguyen, J. Rezessy-Szabó, B. Czukor, A. Hoschke, Continuous production of oligofructose syrup from Jerusalem artichoke juice by immobilized endo-inulinase, Process Biochem. 46 (2011) 298–303, https://doi.org/10.1016/j.procbio.2010.08.028.
[55] G.E.A. Awad, H.R. Wehaid, A.A.A. El Aty, M. Hassan, A novel alginate–CMC gel beads for efficient covalent inulinase immobilization, *Colloid* Polym. Sci. 295 (2017) 495–506, https://doi.org/10.1007/s00396-017-4024-x.
[56] R.S. Singh, R.P. Singh, J.F. Kennedy, Immobilization of yeast inulinase on chitosan beads for the hydrolysis of inulin in a batch system, Int. J. Biol. Macromol. 95 (2017) 87–93, https://doi.org/10.1016/j.ijbiomac.2016.11.030.